Article

Improvement of Municipal Solid Waste Syngas Premixed Flame with Cellular Structure on a Flat Burner

Amornrat Kaewpradap *, Paweenuch Sarmarnjit, Pisit Korkeatkangwan, Kritchaniphat Sawatnuchart and Sumrerng Jugjai

Combustion and Energy Research Laboratory (CERL), Department of Mechanical Engineering, Faculty of Engineering, King Mongkut's University of Technology Thonburi, 126 Pracha Uthit Road, Bang Mod, Thung Khru, Bangkok 10140, Thailand
* Correspondence: amornrat.kae@mail.kmutt.ac.th

Abstract: This research was conducted to study the flame instability of syngas derived from raw municipal solid waste (MSW) and its potential as a natural gas (NG) replacement in power generation. MSW syngas is a mixture of various components such as methane (CH_4), nitrogen (N_2), oxygen (O_2), and hydrogen (H_2), whereas NG is mainly composed of CH_4 (>70%) and CO_2 (>10%). The flame characteristics of these two gases are quite different thus a direct replacement of NG with MSW syngas is impossible. Improvements to MSW syngas combustion are needed through the augmentation of the gas with CH_4 and H_2 active additives at various ratios so that its flame characteristics are comparable to those of NG. A typical MSW syngas composed of 16.2% methane (CH_4), 13.5% hydrogen (H_2), 69.1% nitrogen (N_2), and 0.6% oxygen (O_2) (by vol.) is available in Thailand with great potential for use as an NG replacement. In this study, this gas is used as a representative fuel for improvement and is referred to as simulated Syngas 1. Its premixed flame was studied using a McKenna flat burner to understand its flame instability. Various percentages of CH_4 and H_2 were added to Syngas 1. Its flame characteristics were measured and compared to those of NG. These characteristics included the cellular flame, cell size, flat flame, flammability limit, and flame temperature. The results showed that the flame instability of Syngas 1 was significantly suppressed by adding minimal amounts of CH_4 and H_2. The new composition of Syngas 1 consisted of 19.3% methane (CH_4), 19.0% hydrogen (H_2), 61.2% nitrogen (N_2), and 0.5% oxygen (O_2) (by vol.). It yielded flame characteristics that were comparable to those of an NG flame. This study shows that MSW syngas can potentially replace NG in power generation.

Keywords: municipal solid waste syngas; cellular flame; flame instability; flat burner; natural gas; gasification

1. Introduction

Municipal solid waste (MSW) consists of food waste, yard waste, office paper, corrugated printed newspaper, fruit waste, vegetable peel waste, leaf waste, and leaf litter. Food waste accounts for the majority of the organic components of MSW [1]. In many countries, the current situation of municipal solid waste management (MSWM) has been studied to understand the consequences of untreated waste on humans and the environment and to demonstrate the potential for sustainable management [2]. MSW is a major pollutant and has long been an important issue in Thailand. In 2017, 27.37 million tons of MSW were produced, of which 10.85 and 9.76 million tons were properly managed and recycled, respectively. Moreover, the MSW production per capita has increased to 1.13 kg per person [3]. Currently, the Thailand Department of Renewable Energy Development and Energy Conservation is aiming to increase the proportion of renewable energy utilized and develop capabilities in thermally produced electricity and biofuel power under the Alternative Energy Department Plan 2015 (AEDP 2015). The Ministry of Energy produced

151.6 MW and 191.4 MW of electricity from waste in 2017 and 2018, respectively [4]. In 2021 in line with the AEDP, the total installed capacity of electricity generated using alternative energy was 12,386 MW, which was up 3.2% from the previous year. MSW power plants contributed 388.5 MW or 3.1% of the total installed capacity [5]. MSW has great potential for power generation and can also help to reduce greenhouse gas emissions.

To convert MSW to energy, refuse-derived fuel (RDF) is produced to reduce the moisture content of MSW. Then, mass-burn incineration and waste-to-energy gasification are applied [6]. Mass-burn incineration and gasification can, respectively, convert one ton of MSW into about 550 kWh and 1000 kWh of electricity [7]. The MSW-to-energy process has been improved by plasma gasification technology, which enhances the composition of syngas in terms of its hydrogen content. In Thailand, MSW is refined to one of seven RDF forms, RDF-1 (MSW), RDF-2 (coarse RDF), RDF-3 (fluff RDF), RDF-4 (dust RDF), RDF-5 (densified RDF), RDF-6 (RDF slurry), and RDF-7 (syngas). This reduces the size of the material and removes certain materials that provide alternative fuels for gasification [8]. In the past, plasma-assisted gasification was applied to produce syngas from variations of RDF-5, waste reject (WR), and woodchips (WC) as WC, RDF-5/WC (50–50), RDF-5/WC (70–30), and RDF-5. MSW syngas produced by RDF-5, WR, and WC is primarily composed of N_2, CH_4, H_2, and CO_2. However, the heating value of MSW syngas is too low (4.82–8.26 MJ/Nm^3) to use for power generation according to the AEDP energy plan [9]. Thus, it is crucial to improve MSW syngas for power generation. In a previous study, the carbon conversion efficiency (CCE) and cold gas efficiency (CGE) of MSW syngas were improved using landfill-derived torrefied refuse fuel in a downdraft gasifier. The study aimed to upgrade reclaimed landfill waste to RDF torrefaction to obtain clean syngas in the same gasifier [10]. A multi-stage co-generation system was also used for biomass and MSW to obtain high-quality syngas [11]. Moreover, in another study, the hydrogen (H_2) molar yield during MSW gasification was improved by reusing CO_2 and steam [12]. However, the previous studies focused on the improvement of the MSW syngas process, but improvements to the MSW syngas composition and combustion characteristics, such as its flame stability as a replacement for natural gas in power plant applications, were not investigated.

Generally, power generation almost exclusively uses natural gas (NG) combustion with gas turbines, gas engines, and cogeneration processes due to the low carbon composition of NG and its emissions. According to the Energy Information Administration (EIA), the power generation sector accounted for 37% of total NG usage, which exceeded that of the industrial, residential, commercial, and transportation sectors [13]. However, the high consumption of NG for power generation is a concern. Following the AEDP energy plan, alternative, sustainable energy sources such as MSW syngas should be improved to assure energy security in the future.

In previous research on power generation, the wall temperature of a micro-gas turbine was examined during NG combustion for the development of gas turbine materials and technology [14]. The characteristics and instability of cellular flames in NG from both the western and eastern regions of Thailand were investigated using a McKenna flat burner [15,16]. The pattern formation, turbulence in the flames, and diffusive-thermal theory of cellular flames were reported [17,18]. Flame instability, as indicated by the cell size of a cellular flame, was studied by varying the equivalence ratios. Moreover, the flame instabilities of oxyhydrogen and synthetic biogas were studied [19–21]. The effect of CO_2 addition on the instability of H_2-O_2 combustion flames was investigated. A McKenna flat burner was used to analyze and diagnose the instability of methane–air lean premixed flames [22]. The instability of these premixed flames was influenced by a lower equivalence ratio (lean mixture) and CO_2 addition.

Thus, the improvement of MSW syngas by improving its composition so it can be used as a replacement for natural gas in power plant applications is of great importance. The potential benefits of adding high-heating-value gases such as hydrogen and methane to improve MSW syngas have not yet been studied. In order to determine its suitability for

use as a fuel in power plants, a comparison with the combustion characteristics and flame stability of the main fuels such as natural gas is necessary. McKenna flat burner is a suitable way to test the flames of syngas with different compositions during the combustion of MSW syngas. In the present study, premixed MSW syngas flames are investigated using a McKenna flat burner. This study focuses on the following aspects:

- The cellular flame characteristics and flame stability of MSW syngas;
- The composition of the improved MSW syngas to show that is closer to the flame characteristics of natural gas;
- The cellular flame characteristics and flame stability of the improved MSW syngas.

The contributions of this study are the investigation of the flame characteristics and flame stability of MSW syngas using cellular flames on a McKenna flat burner. Moreover, the study examines the effects of adding methane and hydrogen to MSW syngas to obtain a suitable composition by comparing the resulting flames to the flame characteristics of NG. Improving the composition of MSW syngas is important, as it has the potential to replace NG in power generation as an environmentally friendly solution.

2. Methodology

Table 1 shows the simulated MSW syngas compositions and heating values (LHV_{mixed}) calculated using Equation (1), together with the mixed gaseous ratios (n_a) and heating values of gases (LHV_a) such as CH_4 (35.8 MJ/Nm^3) and H_2 (10.8 MJ/Nm^3). Using the values in Table 1, experimental evaluations of MSW syngas combustion were conducted to study the independent effects of CH_4 and H_2, as well as their combined effects, using a McKenna flat flame. CH_4 and H_2 were added to Syngas 1 to improve its combustion characteristics. Syngas 1 showed the most potential to replace NG owing to its higher composition of combustible gases, CH_4 and H_2. Table 2 shows Syngas 1-C1, Syngas 1-C3, and Syngas 1-C5, which were the Syngas 1 samples to which 1.0%, 3.0%, and 5% of CH_4 were, respectively, added to study the independent effects of CH_4 addition. Similarly, Syngas 1-H7, Syngas 1-C1H7.3, Syngas 1-C3H7.7, and Syngas 1-C5H8 were the Syngas 1 samples to which 7.0% H_2 and 1.0% CH_4, 7.3% H_2 and 3.0% CH_4, 7.7% H_2 and 5.0% CH_4, as well as 8.0% H_2, were added to study the independent effects of H_2 and the combined effects of the addition of CH_4 and H_2. The gas velocity needed to be less than 25 L/min to avoid flashbacks. By limiting the gas flow rate, the effects of CH_4 and H_2, as well as their combined effects, were investigated. The improved MSW syngas combustion flames were analyzed and compared to the flame stability of NG [15]. The factors considered include the flammability limit (at $\Phi \leq 0.61$), flame temperature (1030 °C), and flat flame (at $\Phi \geq 0.70$).

$$LHV_{mixed} = \sum_{a=1}^{N} n_a LHV_a \tag{1}$$

Table 1. Compositions of five simulated MSW syngases.

Syngas	Represented MSW Syngas	Compositions of Simulated Syngas [%Vol.]				*LHV* [MJ/Nm^3]
		CH$_4$	H$_2$	N$_2$	O$_2$	
1	WR10	16.2	13.5	69.1	0.6	7.14
2	WR25	13.4	14.3	71.6	0.7	6.30
3	WR40	7.2	15.2	76.7	0.9	4.20
4	RDF5	7.9	5.0	86.5	0.6	3.34
5	RDF5WC30	10.1	7.1	82.2	0.6	4.35

2.1. Equivalence Ratio

The equivalence ratio (Φ) is the ratio between the actual $\left(\dot{m}_F / \dot{m}_A\right)_{actual}$ and stoichiometric fuel/air mass flow rates $\left(\dot{m}_F / \dot{m}_A\right)_{stoi}$, which are calculated using Equation (2). The fuel mass flow rate ($\dot{m}_F$) and air mass flow rate ($\dot{m}_A$) are the ratios of fuel to air used in this

experiment. The stoichiometry fuel/air mass flow rates are the ratios of fuel to air for a theoretically complete combustion of each MSW syngas.

$$\Phi = \frac{\left(\dot{m}_F / \dot{m}_A\right)_{\text{actual}}}{\left(\dot{m}_F / \dot{m}_A\right)_{\text{stoi}}} \tag{2}$$

Table 2. Compositions of simulated syngas mixtures with the addition of CH_4 and H_2 to Syngas 1.

Syngas	Composition of Addition [%Vol.]		Compositions of Simulated Syngas [%Vol.]				*LHV* [MJ/Nm³]
	CH₄	H₂	CH₄	H₂	N₂	O₂	
1	-	-	16.2	13.5	69.1	0.6	7.14
1-C1	1.0	-	17.6	13.4	68.4	0.6	7.70
1-C3	3.0	-	19.2	13.1	67.1	0.6	8.23
1-C5	5.0	-	20.8	12.8	65.8	0.6	8.77
1-H7	-	7.0	15.7	19.1	64.6	0.6	7.63
1-C1H7.3	1.0	7.3	16.4	19.2	63.8	0.6	7.90
1-C3H7.7	3.0	7.7	17.9	19.2	62.4	0.5	8.43
1-C5H8	5.0	8.0	19.3	19.0	61.2	0.5	8.90

2.2. Adiabatic Flame Temperature (T_{ad})

The adiabatic flame temperature is defined as the balance between the standardized enthalpy of the reactants at the initial state and the standardized enthalpy of the products at the final state [23]. Using the theoretical flame temperature, the energy balance between the enthalpy of the reactant (H_R) and the enthalpy of the product (H_P) is analyzed using Equation (3) and the flame temperature is obtained using Equation (4).

$$H_R = \sum_R N_i \overline{h_i} = H_P = \sum_P N_i \overline{h_i} \tag{3}$$

$$H_P = \sum_R N_i \left[\overline{h_{f,i}^0} + \overline{c_{p,i}} \left(T_{ad} - 298 \right) \right] \tag{4}$$

where
T_{ad} = the adiabatic flame temperature (K);
H_R = the enthalpy of the reactant (kJ);
H_P = the enthalpy of the product (kJ);
N_i = the reactant or product mole;
$c_{p,i}$ = the specific heat (kJ/kmol·K);
$h_{f,i}^0$ = the enthalpy of the formation (kJ/kmol).

2.3. Cell Size of Cellular Flames

The cell size is defined as the distance between the cusps of the cellular flames, D, as shown in Figure 1. The cell size (d, mm) is the relation between the burner diameter (D, mm) and the number of cellular flames (N, cells) due to intrinsic instability. As a cell-size relation, it can be calculated using Equation (5).

$$d = N/D \tag{5}$$

2.4. Power Spectral Density

Following the experimental study, the light emissions of the flames were detected using a photodiode. The intensities of the light emissions were normalized with time and are denoted by $y(t)$. These time series data were analyzed using a fast Fourier transform (FFT) to obtain the relation between the power spectral density and the frequency. A sharp peak (f_1) was also found at a significant oscillation frequency, which was related to the time delay (τ) for a reconstructed attractor.
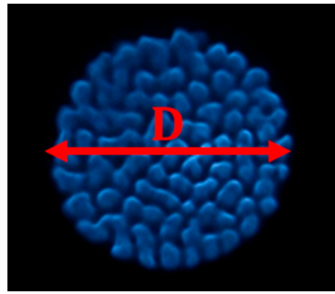
Figure 1. Demonstration of cell size, which is the relation between the burner diameter and the number of cellular flames.

2.5. Reconstructed Attractor

The time series of the light emission intensity $y(t)$ was normalized using an FFT to create an embedding dimension (m) of vector $\vec{V}(t)$ in the time-delayed coordinate. The embedding dimension was 3, as shown in Equation (6). A sharp peak was calculated using Equation (7) to obtain the time delay. Then, the reconstructed attractors were created from the light emission intensities with time delays according to Taken's embedding theorem, as shown in Figure 2 [24].

$$\vec{V}(t) = [y(t), y(t+\tau), y(t+2\tau), \ldots, y(t+(m-1)\tau)] \tag{6}$$

$$\tau = \frac{1}{4f_1} \tag{7}$$
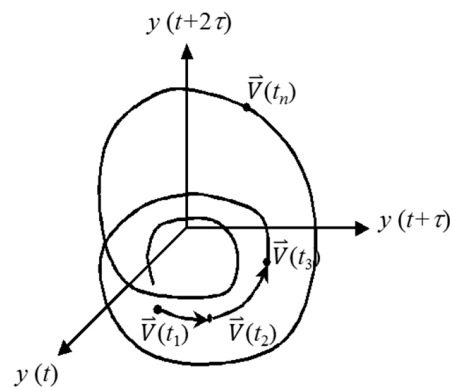
Figure 2. Reconstructed attractor using Taken's embedding theorem [24].

2.6. Municipal Solid Waste (MSW) Syngas

Generally, the main components of MSW syngas obtained from plasma-assisted air gasification are N_2, H_2, and CH_4, as other components, such as CO, CO_2, and O_2, are less abundant. As CO is not permitted for experimentation and there is a limit of four mixing gases for this experiment, the composition of CO and CO_2 is included in the nitrogen composition for this study. In this study, the MSW syngas was obtained from a representative sample of RDF and waste reject (with variations in moisture) as a result of the gasification process [9]. The simulated MSW syngas applied in this study is primarily composed of CH_4, H_2, N_2, and O_2. Based on the MSW syngas compositions [9], there are five typical compositions of MSW syngas with different compositions obtained from a gasification process that need to be improved. Three of the MSW compositions consist of waste reject with 10%wt, 25%wt, and 40%wt of humidity, which are called WR10 (Syngas 1), WR25 (Syngas 2), and WR40 (Syngas 3), respectively. The two other compositions consist of refuse-derived fuel or RDF5 (Syngas 4) and RDF5 with 30% wood chips or RDF5WC30 (Syngas 5). In this study, however, the compositions of the five typical MSW syngas types

were simulated, as shown in Table 1. The effect of the CH_4 composition can be studied by comparing the results using Syngas 2 and Syngas 3, whereas the effect of H_2 is observed by the difference in the results between Syngas 3 and Syngas 4.

2.7. Natural Gas Composition

In this study, the composition of synthetic NG is represented by 89% CH_4 and 11% CO_2 [15]. The combustion flame characteristics of the synthetic NG were investigated to obtain the flammability limit or blow-off limit, flame temperature, and flat flame.

3. Experimental Setup

3.1. McKenna Flat Burner

A McKenna flat burner is made using sintered metal with 46.5% porosity and a diameter of 60 mm, as shown in Figure 3. This flat burner is equipped with a water-cooling system to prevent overheating and flame flashback. A flat flame can be completely induced above the surface of the flat burner without a radiation effect due to the uniform flow and the lack of a flame curvature. Notably, the McKenna flat burner can provide baseline data for flames. Thus, it is very valuable for the comparison of flames and the assessment of the combustion performance of fuel.
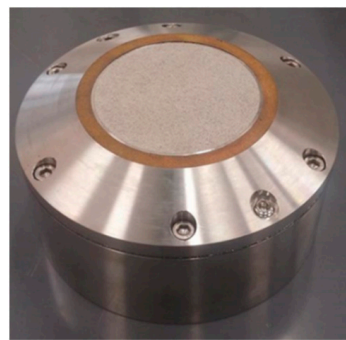

Figure 3. McKenna flat burner used in the current study.

3.2. Experimental Apparatus

The experimental setup for MSW syngas combustion is shown in Figure 4. The simulated MSW syngas and air were metered using a digital mass flow controller before entering a mixing chamber. The mixture of MSW syngas (CH_4, H_2, N_2) and air from the mixing chamber was then ignited at the surface of the 60 mm diameter McKenna flat burner to produce a cellular flame. The total flow rate of the mixture was set at 25 L/min. A digital camera (Nikon DSLR D7100) was used to take photographs of the cellular flames. The light emissions were measured using a photodiode (HAMAMATSU S1223-01). The output current from the photodiode was recorded using a Photosensor Amplifier (Hamamatsu C9329) and data logger (Hioki LR8431-20) with a 100 Hz sampling frequency.
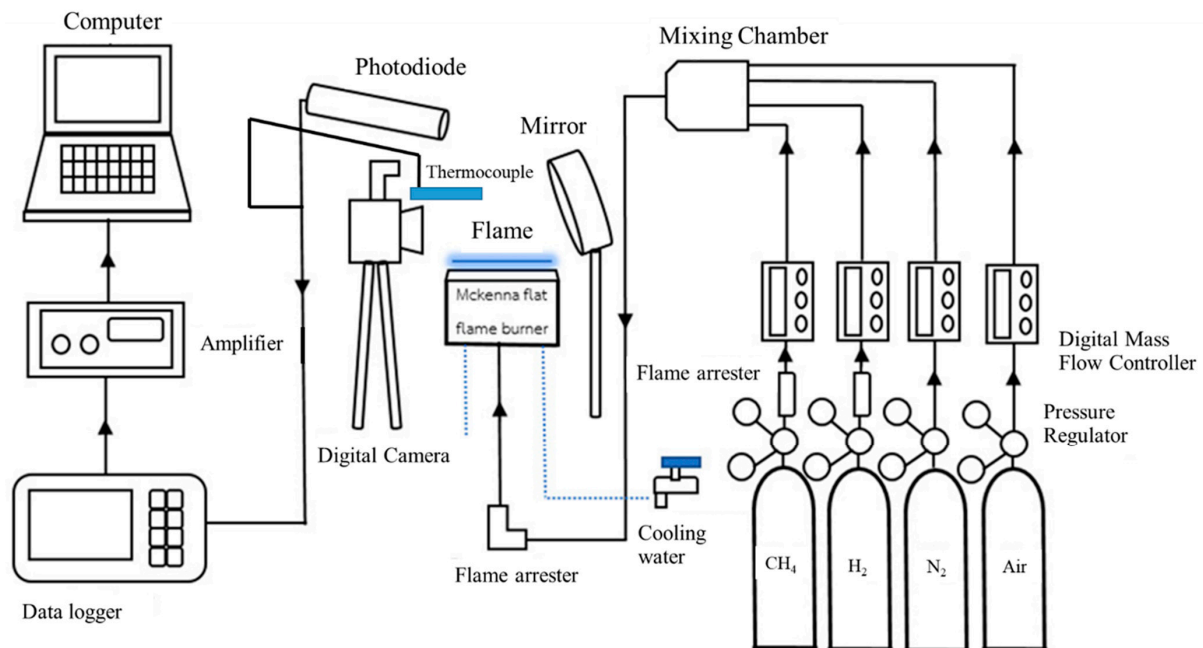
Figure 4. Experimental apparatus of the current study.

4. Results and Discussion

4.1. Combustion Characteristics of Simulated MSW Syngas

Figure 5 shows images of the cellular flames of the simulated MSW syngas samples described in Table 1. The simulated MSW syngas samples (Syngas 1–5) were fed into a McKenna flat burner at a constant flow rate of 25 L/min and Φ = 0.6, 0.7, 0.8, 0.9, and 1.0. The results showed that Syngas 4 and Syngas 5 could not be ignited, and no combustion flames were observed. Only Syngas samples 1–3 were ignited to yield cellular flames. When the equivalence ratio was approximately 1, flat flames with small cellular flames combined into a single flat flame formed in every syngas due to the flame stability. Alternatively, cellular-like structure flames were formed when the cell size became larger at lower equivalence ratios due to thermally diffusive instability. Figure 5 also shows that flame blow-off occurred at $\Phi < 0.6$ for each syngas. At $\Phi = 0.8$, the cell size of Syngas 1 was relatively smaller compared to those of Syngas 2 and Syngas 3. At a higher equivalence ratio, Syngas 1 produced a flat flame and a wider range of blow-off flames due to the strengthening of the flame stability.
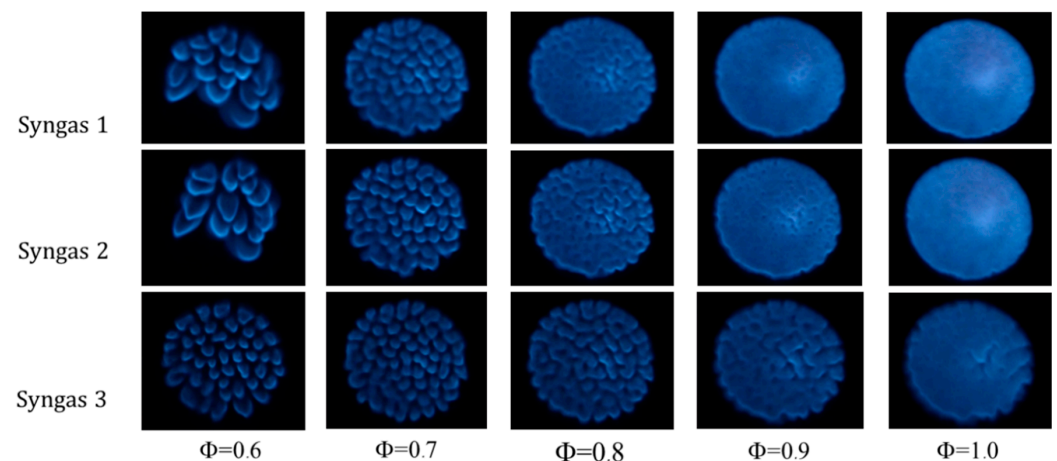

Figure 5. Images of cellular flames from Syngas 1, Syngas 2, and Syngas 3 at Φ = 0.6, 0.7, 0.8, 0.9, and 1.0.

Figures 6–8, respectively, show the corresponding power spectral density variations with Φ = 0.6, 0.8, and 1.0 for Syngas 1, Syngas 2, and Syngas 3. When the equivalence ratio was higher (Φ = 1.0), a higher peak frequency and power spectral density were obtained. The comparison of Syngas samples 1–3 showed a lower sharp peak frequency and power spectral density. Then, the lower sharp peak frequency was analyzed, and a wider range of time delays and greater attractors were observed due to instability, as shown in Figures 9–11. At Φ = 1.0, the flat flames and higher power spectral density resulted in the reconstructed attractor with small points. The reconstructed attractors were greater and more complex for Syngas 3 because of the intensity of the instability.
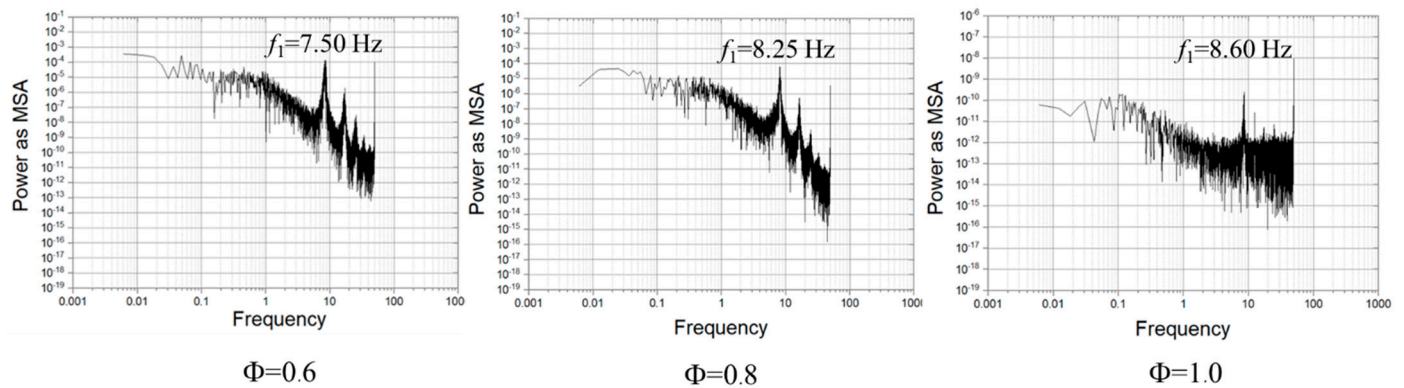
Figure 6. Power spectral density of Syngas 1 at Φ = 0.6, 0.8, and 1.0.
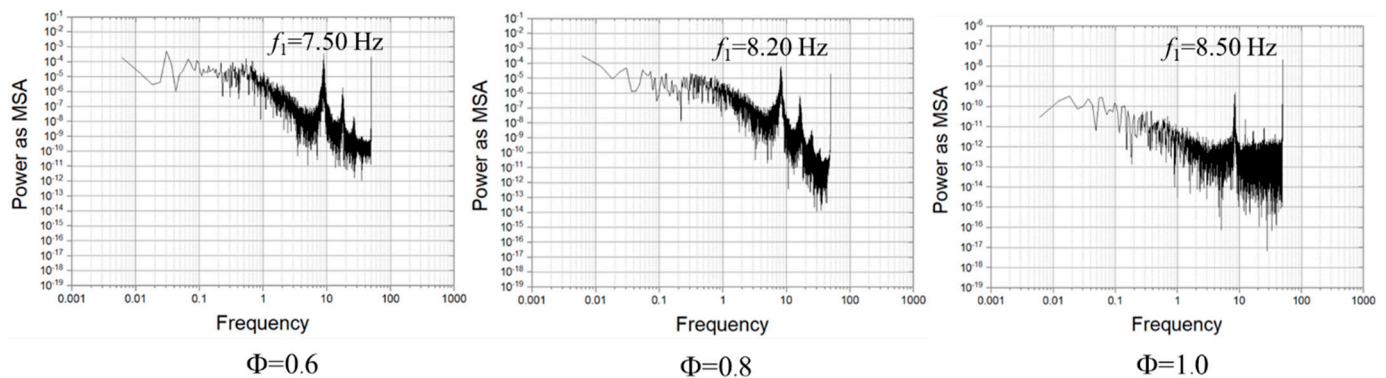

Figure 7. Power spectral density of Syngas 2 at Φ = 0.6, 0.8, and 1.0.
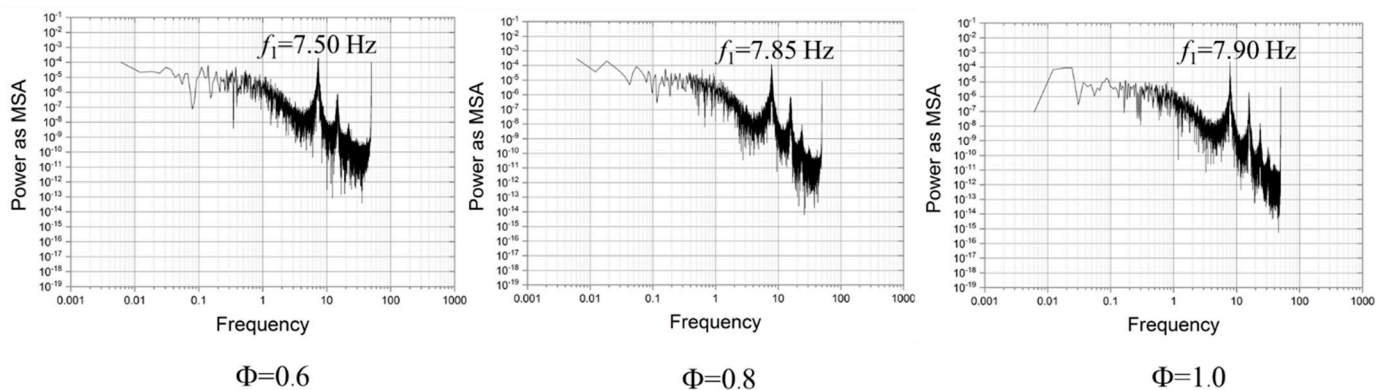

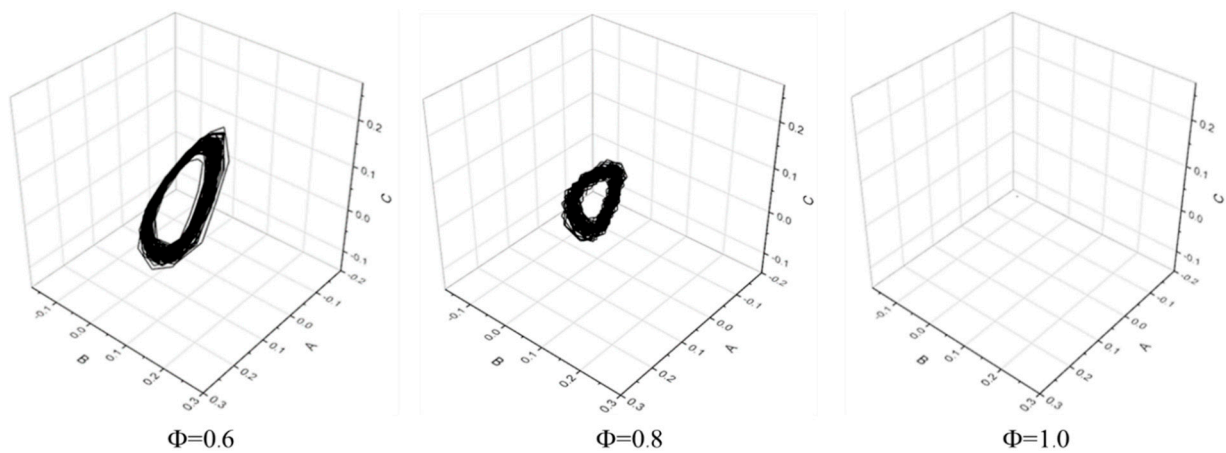**Figure 8.** Power spectral density of Syngas 3 at Φ = 0.6, 0.8, and 1.0.

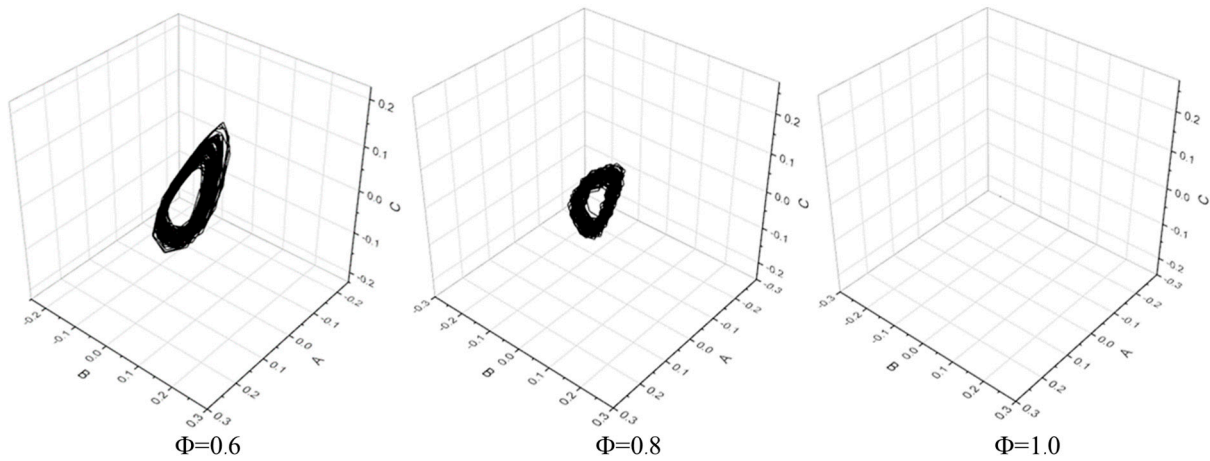**Figure 9.** Reconstructed attractor of Syngas 1 at Φ = 0.6, 0.8, and 1.0.

Figure 10. Reconstructed attractor of Syngas 2 at Φ = 0.6, 0.8, and 1.0.
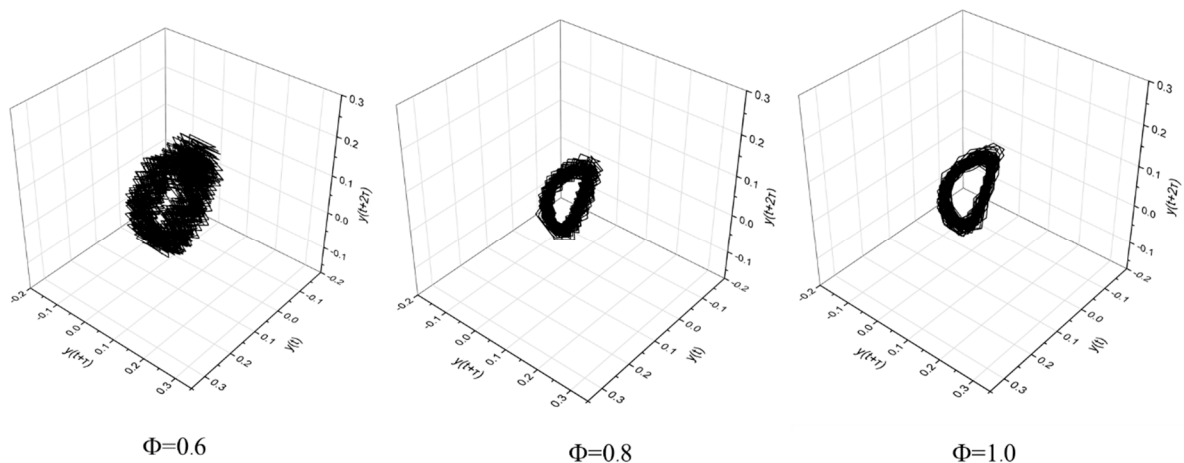

Figure 11. Reconstructed attractor of Syngas 3 at Φ = 0.6, 0.8, and 1.0.

4.2. Effect of CH_4 on Cellular Flames

CH_4, among other hydrocarbon fuels, has the maximum hydrogen-to-carbon ratio. It can be used as an active additive to improve the burning velocity, flame temperature, and flame stability of fuel. The effect of CH_4 can be studied by comparing the reconstructed attractors of Syngas 2 and Syngas 3, as shown in Figures 10 and 11. At Φ = 1.0, Syngas 2, with a comparatively high CH_4 content, yielded a flat flame with a relatively small point

attractor, as opposed to that of Syngas 3. Thus, the addition of CH_4 to any syngas can effectively induce a flat flame with enhanced flame stability.

4.3. Effect of H_2 on Cellular Flames

Theoretically, hydrogen has the highest energy density because it is the lightest element. Moreover, hydrogen consists entirely of single-bonded hydrogen atoms, which is due to a linear branching chain reaction resulting in an enhanced combustion reaction [25]. To analyze the H_2 effect, the combustion characteristics of Syngas 4 (5.0% of H_2) and Syngas 3 (15.2% of H_2) were examined. The ignition and combustion flames from Syngas 3 were observed, whereas those of Syngas 4 were not. Thus, an increased H_2 composition can enhance the flammability limit or blow-off flame range, as shown in Figure 5. However, a more stable flame, such as a flat flame, was not achieved with a higher H_2 level.

4.4. Improvement of Syngas 1 with the Addition of CH_4 and H_2

In Table 2, it can be seen that Syngas 1 was improved by the addition of CH_4 and H_2. The improvement of Syngas 1 was achieved with the addition of CH_4 at various quantities (as a volume percentage of the original composition of Syngas 1). This produced Syngas 1-C1, Syngas 1-C3, and Syngas 1-C5, where C represents CH_4 and the numeric value after C is the percentage (by volume) of the CH_4 addition. For example, Syngas 1-C1 is Syngas 1 with the addition of 1.0% of CH_4 to its original composition.

Figure 12 shows images of the cellular flames of Syngas 1, Syngas 1-C1, Syngas 1-C3, and Syngas 1-C5 at Φ = 0.6–1.0. The addition of CH_4 to Syngas-1 was very effective in enhancing its combustion.
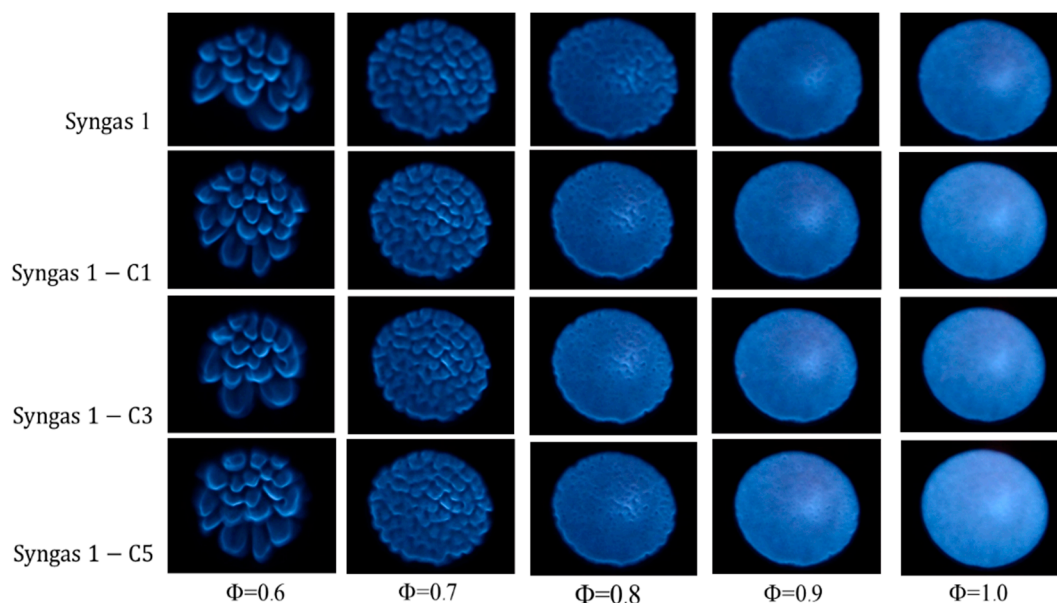

Figure 12. Cellular flames of Syngas 1, Syngas 1-C1, Syngas 1-C3, and Syngas 1-C5 at Φ = 0.6–1.0.

For Syngas 1, a flat flame was observed at Φ = 1.0. When the CH_4 addition increased, flat flames were observed at Φ = 0.9 for Syngas 1-C3 and Syngas 1-C5 due to flame stability.

At Φ = 0.8, the CH_4 composition increased, the apparent cell size decreased, and the cells almost combined into a flat flame owing to the enhanced burning velocity, flame temperature, and flame stability. The apparent cell size was also strongly dependent on the value of Φ. It became smaller as the equivalence ratio increased owing to improved flame stability.

Figures 13–15 show the corresponding reconstructed attractors of Syngas 1-C1, Syngas 1-C3, and Syngas 1-C5. The smaller or smoother the reconstructed attractor of the flame, the more stable the associated cellular flame. The effectiveness of the addition of CH_4 to

Syngas 1 for combustion improvement was confirmed by comparing the reconstructed attractors. At $\Phi = 0.8$, a larger reconstructed attractor was observed for Syngas 1-C1, whereas smaller ones were observed for Syngas 1-C3 and Syngas 1-C5. Moreover, a smoother doughnut ring of the reconstructed attractor from Syngas 1-C5 was observed compared to that of Syngas 1-C3 at $\Phi = 0.6$. The size of the reconstructed attractor was strongly dependent on the value of Φ. The reconstructed attractor became smaller as the equivalence ratio increased due to the effective improvement in the flame stability with the addition of CH_4.
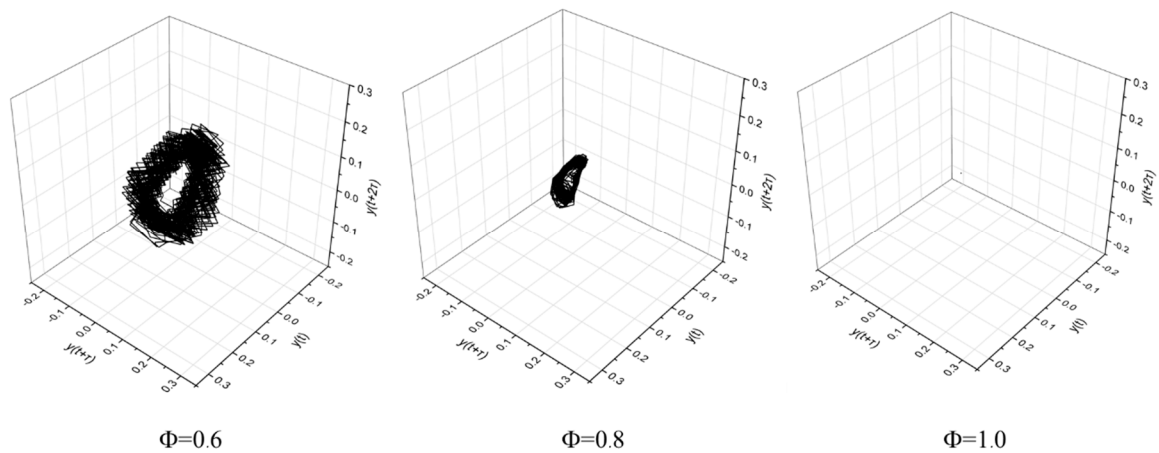

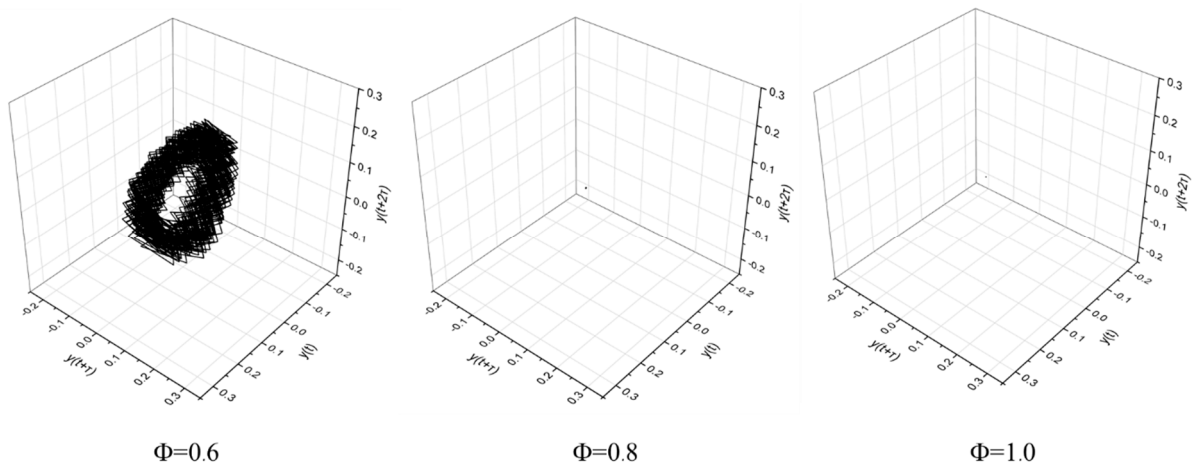**Figure 13.** Reconstructed attractor of Syngas 1-C1 at $\Phi = 0.6$, 0.8, and 1.0.

Figure 14. Reconstructed attractor of Syngas 1-C3 at $\Phi = 0.6$, 0.8, and 1.0.
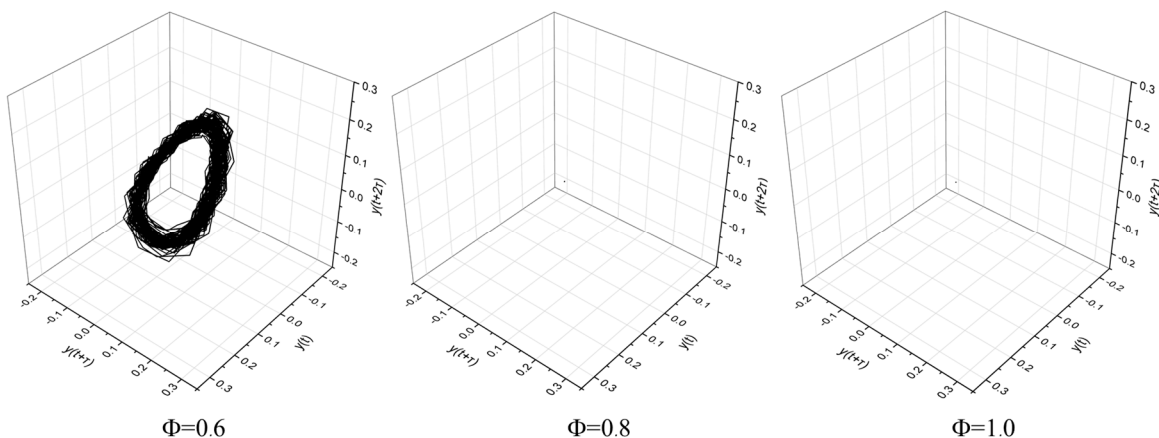

Figure 15. Reconstructed attractor of Syngas 1-C5 at $\Phi = 0.6$, 0.8, and 1.0.

Figure 16 shows the cellular flames of Syngas 1-H7, Syngas 1-C1H7.3, Syngas 1-C3H7.7, and Syngas 1-C5H8 at Φ = 0.6–1.0. Further improvements were achieved by separately or simultaneously adding CH_4 and H_2 to Syngas 1. This resulted in Syngas 1-H7, Syngas 1-C1H7.3, Syngas 1-C1H7.3, Syngas 1-C3H7.7, and Syngas 1-C5H8, where H represents hydrogen, and the numeric value is the percentage (by volume) of hydrogen added to the original Syngas 1. The cell size of NG is also shown for comparison. Again, the apparent cell size was also strongly dependent on the value of Φ. The cell size was inversely proportional to the equivalence ratio. It was higher when the equivalence ratio was lower, and the flame blew off if Φ was less than 0.6. At Φ = 0.8–1.0, flat flames were observed for both NG and all of the improved syngas flames due to greater flame stability.
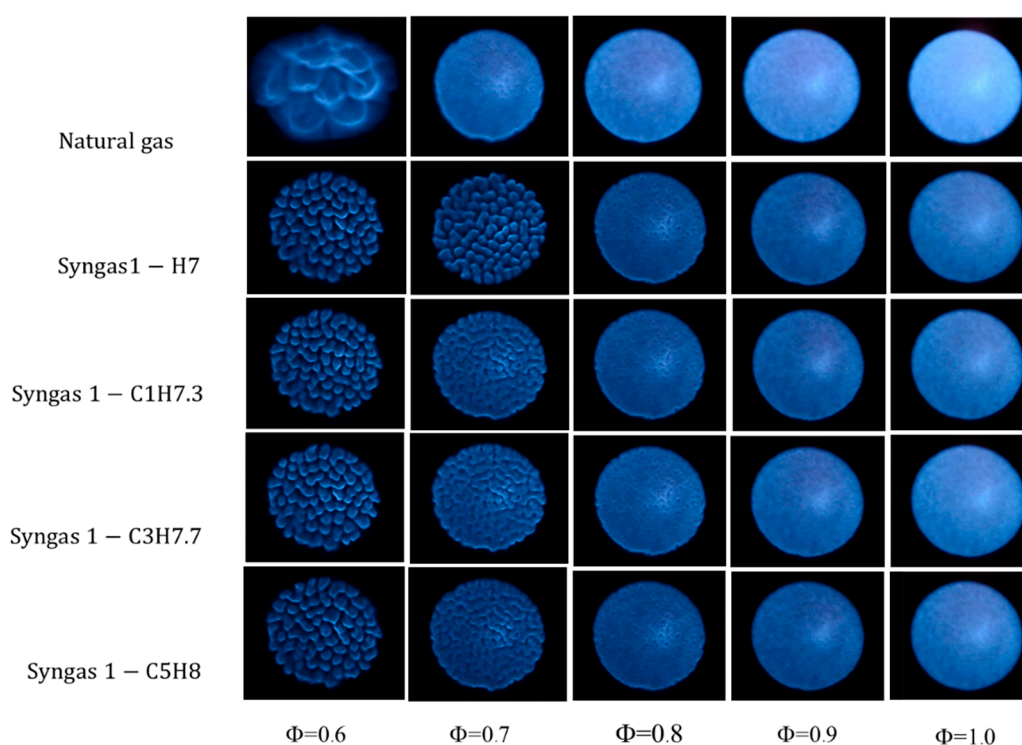

Figure 16. Cellular flames of natural gas [15] and Syngas 1 with the addition of H_2 and CH_4, which created Syngas 1-H7, Syngas 1-C1H7.3, Syngas 1-C3H7.7, and Syngas 1-C5H8 at Φ = 0.6–1.0.

The effect of the addition of H_2 to syngas can be clearly seen by comparing the apparent cell size of Syngas 1-H7 (Figure 16) to that of Syngas 1 (Figure 15). Similarly, the effect of the addition of H_2 was also determined by comparing the apparent cell size of Syngas 1-H7 (Figure 17) to that of NG [15] (Figure 17). It was clear that the addition of H_2 significantly enhanced the combustion of Syngas 1. Syngas 1-H7 yielded a relatively small cell size compared to those of Syngas-1 and NG [15] over the range of Φ values studied. The typical values of the cell sizes of the various syngas samples were computed and compared at Φ = 0.6, as shown in Table 3. Syngas 1-H7, with a cell size of 7.3 mm, confirmed the effectiveness of the addition of H_2 to Syngas 1. More stable combustion was achieved with a finer cell size. NG [15] showed a relatively large cell size of 19.8 mm, whereas Syngas 1 showed an intermediate cell size of 7.5 mm, as shown in Table 3.

Figure 18 shows the corresponding equivalence ratios at which the first flat flame was observed for each syngas considered in the present study. As the flame stability testing proceeded, the first flat flames were observed from Syngas 1, Syngas 1-C5, and Syngas 1-C5H8, respectively, at Φ = 0.9, Φ = 0.8, and Φ = 0.75. The obtained results showed that the addition of CH_4 to any syngas could effectively induce a flat flame with enhanced flame stability. Although the H_2 addition had no effect on the flat flame, the addition of CH_4 and H_2 enhanced the flat flame and flame instability. Thus, Syngas 1-C5H8 produced the first

flat flame, which appeared at almost the same Φ as that of NG [15], i.e., $\Phi = 0.7$. Figure 19 shows the corresponding equivalence ratios at which the blow-off limit was observed for each syngas considered in the current study. The addition of CH_4 to Syngas 1, i.e., Syngas 1-C1, Syngas 1-C3, and Syngas 1-C5, slightly improved the blow-off limit at $\Phi = 0.58$ compared to Syngas 1 (blow-off limit at $\Phi = 0.6$). However, the addition of CH_4 and H_2 to Syngas 1 significantly improved the blow-off limit at $\Phi = 0.48$. Therefore, the flammability limit of each syngas considered in the current study can be successfully improved to values lower than that of NG (blow-off limit at $\Phi = 0.6$) [15].
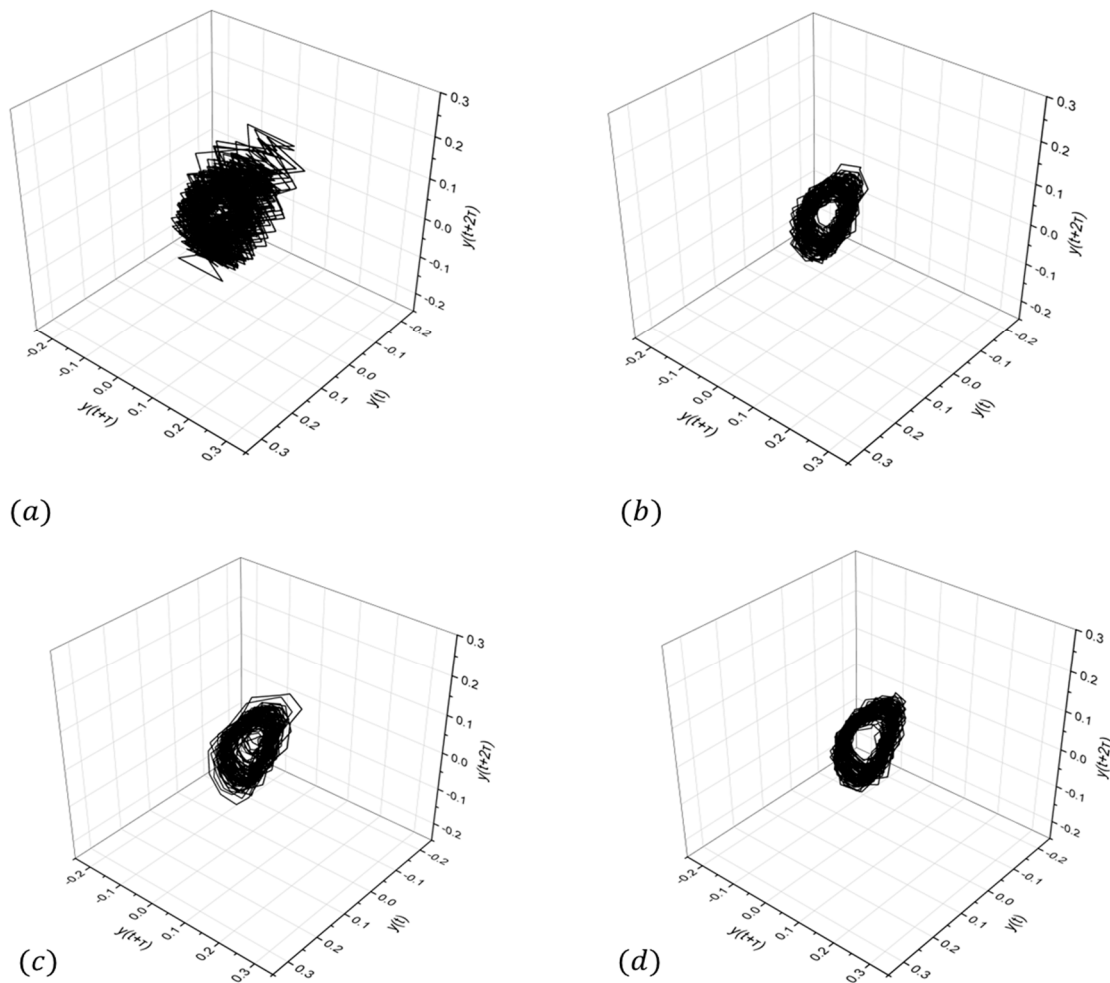

(a)

(b)

(c)

(d)

Figure 17. Typical reconstructed attractors at $\Phi = 0.6$ for (**a**) Syngas 1-H7, (**b**) Syngas 1-C1H7.3, (**c**) Syngas 1-C3H7.7, and (**d**) Syngas 1-C5H8.

Table 3. Typical cell sizes of cellular flames of natural gas [15], Syngas 1 with the addition of H_2 and CH_4, which created Syngas 1-H7, Syngas 1-C1H7.3, Syngas 1-C3H7.7, and Syngas 1-C5H8 at $\Phi = 0.6$.

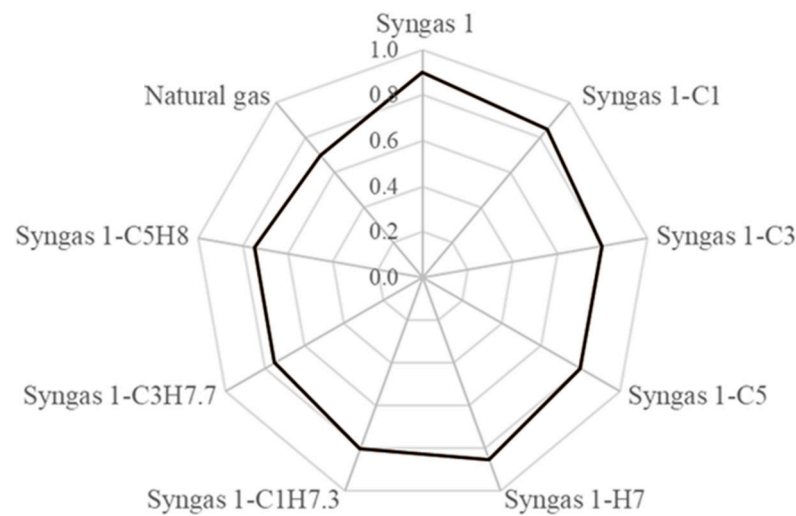| Syngas	*d* (mm)
Natural gas [15]	19.8
1	7.5
1-H7	7.3
1-C1H7.3	6.8
1-C3H7.7	7.0
1-C5H8	6.4

Figure 18. The equivalence ratios of the first flat flame observed from Syngas 1, Syngas 1-C1, Syngas 1-C3, Syngas 1-C5, Syngas 1-H7, Syngas 1-C1H7.3, Syngas 1-C3H7.7, Syngas 1-C5H8, and NG [15].
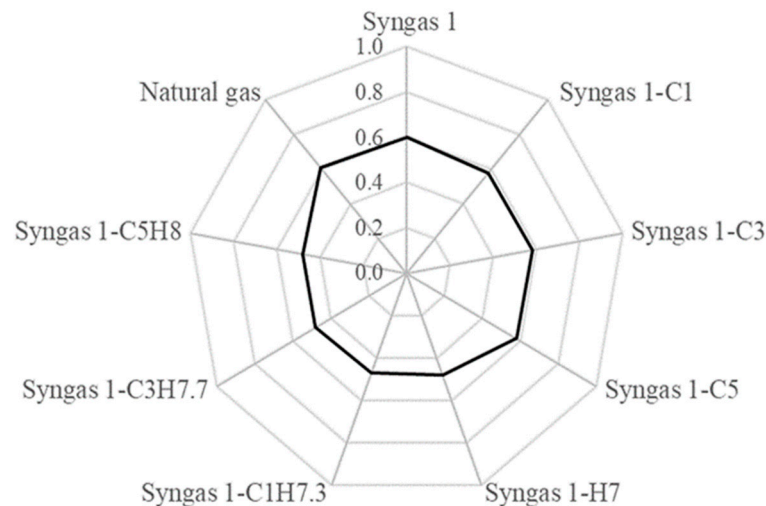

Figure 19. The equivalence ratios of the blow-off flame observed from Syngas 1, Syngas 1-C1, Syngas 1-C3, Syngas 1-C5, Syngas 1-H7, Syngas 1-C1H7.3, Syngas 1-C3H7.7, Syngas 1-C5H8, and NG [15].

Figure 20 shows the typical flame temperatures of Syngas 1, Syngas 1-C1, Syngas 1-C3, Syngas 1-C5, Syngas 1-H7, Syngas 1-C1H7.3, Syngas 1-C3H7.7, Syngas 1-C5H8, and NG at $\Phi = 1.0$. When the addition of CH_4 was higher, as in Syngas 1-C1, Syngas 1-C3, and Syngas 1-C5, the flame temperature increased due to the maximum hydrocarbon ratio effects. Among these, Syngas 1-C5H8 yielded the highest flame temperature, which was close to that of NG [15]. The addition of CH_4 to any syngas could effectively induce a flat flame with enhanced flame stability. Although the H_2 addition did not affect the flat flame, the addition of CH_4 and H_2 enhanced the flat flame and flame instability.

The addition of CH_4 and H_2 to Syngas 1 resulted in Syngas 1-C5H8 with a composition of 19.3% CH_4, 19.0% H_2, 61.2% N_2, and 0.5% O_2 (by vol.), which the lower heating value increased to 8.90 MJ/Nm^3. However, the lower heating value of Syngas 1-C5H8 was lower compared to NG (36.60 MJ/Nm^3). This significantly improved the flame stability in terms of the cell size and reconstructed attractor. The flame characteristics, such as the flat flame, flammability limit, and flame temperature, of the improved Syngas1-C5H8 were comparable to those of NG [15].
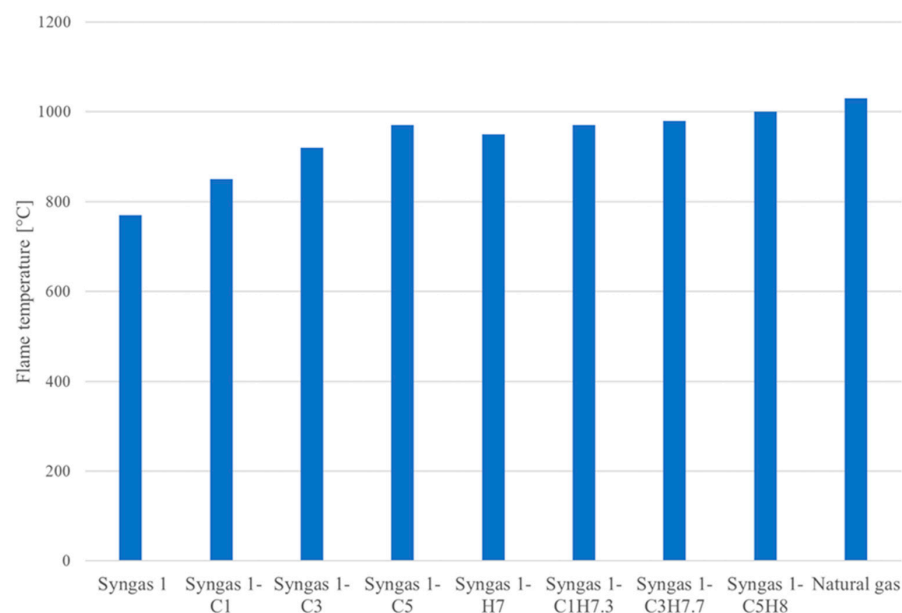
Figure 20. Typical flame temperatures of Syngas 1, Syngas 1-C1, Syngas 1-C3, Syngas 1-C5, Syngas 1-H7, Syngas 1-C1H7.3, Syngas 1-C3H7.7, Syngas 1-C5H8, and NG [15] at $\Phi = 1.0$.

5. Conclusions

The flame instabilities of five simulated municipal solid waste syngas types (MSW syngas) in Thailand were experimentally studied using a McKenna flat burner. In this study, they are referenced as Syngases 1-5, each of which was composed of different concentrations of CH_4, H_2, N_2, and O_2. Further improvements to the flame stability of a selected MSW syngas (Syngas 1) were achieved with the addition of active CH_4 and H_2 to evaluate it as a potential replacement for NG in power generation. The concentrations of CH_4 and H_2 in Syngas 1 were varied and the lower heating value and the flame characteristics, including the cellular flame, cell size, flat flame, flammability limit, and flame temperature, were measured and compared to those of NG. The results of the study are as follows:

1. Not every simulated MSW syngas was ignitable. Syngas 4 and Syngas 5 could not be ignited, whereas Syngas 1, Syngas 2, and Syngas 3 were ignitable, but further improvements to their flame stabilities are required.
2. Among the ignitable syngas samples, Syngas 1, with a composition of 16.2% CH_4, 13.5% H_2, 69.1% N_2, and 0.6% O_2 (by vol.), was the most suitable for further flame stability improvements. This was due to its relatively high concentrations of CH_4 and H_2 compared to Syngas 2 and Syngas 3.
3. The equivalence ratio was an important parameter that controlled flame stability via the cell size of the flame. The cell size was inversely proportional to the equivalence ratio. The cell size was greater when the equivalence ratio was lower, and the flame blew off if Φ was less than a critical value.
4. CH_4 and H_2 can be considered effective additives for improved flame stability. The addition of CH_4 and H_2 to Syngas 1 effectively improved its flame characteristics to a degree comparable to NG. The improved Syngas 1 yielded an increase of 24.6% of the heating value and comparable flame characteristics to those of an NG flame. This study shows that MSW syngas has great potential to replace NG in power generation.

Author Contributions: Conceptualization, A.K. and S.J.; methodology, A.K.; software, P.S., P.K. and K.S.; validation, P.S., P.K. and K.S.; formal analysis, A.K.; investigation, A.K.; resources, A.K.; data curation, P.S., P.K. and K.S.; writing—original draft preparation, A.K.; writing—review and editing, A.K. and S.J.; visualization, A.K.; supervision, A.K. and S.J.; project administration, A.K.; funding acquisition, A.K. All authors have read and agreed to the published version of the manuscript.

Data Availability Statement: Not applicable.

Conflicts of Interest: The authors declare no conflict of interest.

References

1. Wastes-Non-Hazardous Waste-Municipal Solid Waste, Municipal Solid Waste. 2022. Available online: https://archive.epa.gov/epawaste/nonhaz/municipal/web/html/ (accessed on 20 January 2022).
2. Fernandes, R.S.; Shetty, N.S.; Thimmappa, B.H.S. A review of the current situation of municipal solid waste management in India and its potential for anaerobic digestion. *Int. J. Environ. Pollut.* **2022**, *69*, 130–150. [CrossRef]
3. PCD (Pollution Control Department). Municipal Solid Waste Report in Thailand 2017. 2017. Available online: http://www.pcd.go.th/Info_serv/File/WasteSociety60.pdf (accessed on 20 January 2022).
4. Ministry of Energy. Alternative Energy Development Plan 2014–2036. In Proceedings of the Thai-German Technology Conference, Biogas, Thailand, 3–6 June 2015.
5. Ministry of Energy, Thailand. Thailand Alternative Energy Situation 2021. Available online: https://www.dede.go.th/download/state_65/Thailand%20Alternative%20Energy%20Situation%202021_compressed.pdf (accessed on 20 January 2022).
6. Patcharavongsiri, M.; Tondee, T.; Teekasap, S. Process of changing municipal solid waste into RDF using rotary bio-drying. *J. Renew. Energy Smart Grid Technol.* **2019**, *14*, 49–60.
7. Global Syngas Technology Council. Waste to Energy Gasification. 2022. Available online: https://globalsyngas.org/syngas-technology/syngas-production/waste-to-energy-gasification (accessed on 31 January 2022).
8. Ryokusan. 2010. Available online: https://www.ryokusanasia.com (accessed on 31 January 2022).
9. Hinsui, T.; Arjharn, W.; Liplap, P. Plasma-assisted gasification of waste rejected waste from an MBT plant for syngas production. *Suranaree J. Sci. Technol.* **2014**, *22*, 183–196.
10. Laohalidanond, K.; Kerdsuwan, S.; Burra, K.R.G.; Li, J.; Gupta, A.K. Syngas Generation from Landfills Derived Torrified Refuse Using a Downdraft Gasifier. *J. Energy Resour. Technol.* **2021**, *143*, 052102-1–052102-8. [CrossRef]
11. Hu, Y.; Pang, K.; Cai, L.; Liu, Z. A multi-stage co-gasification system of biomass solid waste (MSW) for high quality syngas production. *Energy* **2021**, *221*, 119639. [CrossRef]
12. Zheng, X.; Ying, Z.; Wang, B.; Chen, C. Hydrogen, and syngas production from municipal solid waste (MSW) gasification via reusing CO_2. *Appl. Therm. Eng.* **2018**, *144*, 242–247. [CrossRef]
13. Use of Natural Gas. Energy Information Administration (EIA). 2021. Available online: https://www.eia.gov/energyexplained/natural-gas/use-of-natural-gas.php (accessed on 31 January 2022).
14. Gvozdenac, D.; Menke, C.; Vallikul, P.; Petrovic, J.; Gvodenac, B. Assessment of potential for natural gas-based cogeneration in Thailand. *Energy* **2009**, *34*, 465–475. [CrossRef]
15. Kaewpradap, A.; Jugjai, S. Experimental study of flame stability enhancement on lean premixed combustion of a synthetic natural gas in Thailand. *Energy* **2019**, *188*, 116029. [CrossRef]
16. Wright, I.G.; Gibbon, T.B. Recent developments in gas turbine materials and technology and their implications for syngas firing. *Energy* **2007**, *32*, 3160–3621. [CrossRef]
17. Sivashinsky, G. Instabilities, pattern formation, and turbulence in flames. *Annu. Rev. Fluid Mech.* **1983**, *15*, 179–199. [CrossRef]
18. Sivashinsky, G. Diffusive-thermal theory of cellular flames. *Combust. Sci. Technol.* **1977**, *15*, 137–145. [CrossRef]
19. Kaewpradap, A.; Kadowaki, S. Instability Influenced by CO_2, and Equivalence Ratio in Oxyhydrogen Flames on Flat Burner. *Combust. Sci. Technol.* **2017**, *189*, 438–452. [CrossRef]
20. Konnov, A.A. Model of Cellular Instability of Flames of Ternary Mixtures. *Combust. Explos. Shock. Waves* **2005**, *41*, 496–503. [CrossRef]
21. Kaewpradap, A.; Noppharatana, A.; Jugjai, S. Cellular Premixed Flames of Synthetic Biogas Composition Effects on Flat Burner. *Engineering* **2017**, *21*, 415–425. [CrossRef]
22. Kadowaki, S.; Ohkura, N. Time series analysis on the emission of light from methane-air lean premixed flames: Diagnostics of the flame instability. *Trans. Jpn. Soc. Aeronaut. Space Sci.* **2008**, *51*, 133–138. [CrossRef]
23. Stephen, R. *Turns, An Introduction to Combustion Concepts and Applications*, 3rd ed.; McGraw Hill: New York, NY, USA, 2012; pp. 33–35.
24. Takens, F. Detecting strange attractors in turbulence. In *Dynamical Systems and Turbulence, Lecture Notes in Mathematics*; Rand, D.A., Young, L.-S., Eds.; Springer: Berlin, Germany, 1981; Volume 898, pp. 366–381.
25. Straight-Chain and Branched Alkanes-Chemistry LibreTexts, NICE CXone Expert. Available online: https://status.libretexts.org (accessed on 31 January 2022).